Original Article/นิพนธ์ต้นฉบับ

Diagnostic Accuracy of Multiparametric Magnetic Resonance Imaging in Peripheral Zone Prostate Cancer Detection

Pornphan Wibulpolprasert[1], Sasiprapa Rongthong[1], Sith Phongkitkarun[1], Panas Chalermsanyakorn[2]

[1] *Department of Diagnostic and Therapeutic Radiology, Faculty of Medicine Ramathibodi Hospital, Mahidol University, Bangkok, Thailand*

[2] *Department of Pathology, Faculty of Medicine Ramathibodi Hospital, Mahidol University, Bangkok, Thailand*

Abstract

Background: Multiparametric magnetic resonance imaging (mp-MRI) has emerged as the best noninvasive imaging modality for prostate cancer detection, grading, staging, and targeted biopsy guidance. Validate performance of mp-MRI for peripheral zone prostate cancer detection is important for clinical implication.

Objective: To determine the accuracy of T2-weighted (T2W) imaging, diffusion-weighted imaging (DWI), three dimensional (3D) magnetic resonance spectroscopic (MRS), and dynamic contrast-enhanced imaging (DCE) in peripheral zone prostate cancer detection.

Methods: The retrospective study included 38 patients who has undergone pre-operative endorectal MRI from March 2006, to March 2010. The correlation of T2W, DWI, MRS, and DCE in differentiation between tumor and non-tumor areas were analyzed by using Pearson's chi-square test or Fisher's exact test. The receiver operating characteristic (ROC) analysis was use to evaluate the distinguishing ability of T2W, DWI, MRS, DCE, and the combinations in tumor detection.

Results: In 76 lesions from 38 patients, the area under the ROC curve (AUC) for tumor detection was 0.86 (T2W), 0.86 (DWI), 0.95 (MRS), and 0.61 (DCE). Combination of T2W+DWI, T2W+MRS, T2W+DCE achieved an AUC of 0.86, 0.92, and 0.80, respectively. There is no statistically significant difference in AUC between combination of T2W+DWI (0.86), and combination of T2W+DWI+DCE (0.82), T2W+DWI+MRS (0.81), or T2W+DWI+MRS+DCE (0.78).

Conclusions: DWI is the most useful complementary sequence to conventional anatomical T2W imaging for prostate cancer foci identification. The 3D-MRS and DCE images may be use as confirmation tools in peripheral zone prostate cancer detection.

Keywords: Prostate cancer, Peripheral zone, Multiparametric MRI, Diagnostic accuracy

Corresponding Author: Pornphan Wibulpolprasert

Department of Diagnostic and Therapeutic Radiology, Faculty of Medicine Ramathibodi Hospital, Mahidol University, 270 Rama VI Road, Ratchathewi, Bangkok 10400, Thailand.

Telephone: +66 2201 1212 Fax: +66 2201 1297 E-mail: punlee77@gmail.com, pornphan.wib@mahidol.ac.th

Introduction

Diagnosis of prostate cancer is problematic worldwide, and being the most common cancer diagnosed in Western men in 2015.[1] Over the past few years, functional magnetic resonance imaging (MRI) techniques have been developed to improve the diagnostic accuracy of prostate cancer.[2] MRI of the prostate with a combined pelvic and endorectal coil has become an accepted method for prostate cancer staging.[3] Combination of morphologic and metabolic data in MR spectroscopic (MRS) imaging has demonstrated improvement in tumor detection and better determine grading, staging as well as volume of prostate cancer.[4] It has been well established as the MRS improve the specificity than conventional MRI for prostate cancer localization based on the choline peak elevation and high ratio of choline and creatine to citrate in prostate cancer tissue.[5]

Diffusion-weighted imaging (DWI) with quantitative DWI derivative (apparent diffusion coefficient [ADC]) is a functional imaging technique that quantified the net displacement of water molecules in the tissue and across tissue. Increased cellularity and cell membrane in prostate cancer causes restricted diffusion at high b values, contrast to the normal glandular tissue in peripheral zone.[6, 7] This technique increases sensitivity and accuracy for prostate cancer detection compared to conventional MR sequences[8-10] and able to be a noninvasive biomarker for determining prostate cancer aggressiveness.[11, 12]

The dynamic contrast-enhanced magnetic resonance imaging (DCE-MRI) is based on increased number of abnormal blood vessels and increased permeability as well as extravasation of the contrast agent in interstitium especially in aggressive prostate cancer.[13] The vascularity of solid tumors show earlier and more pronounced enhancement than surrounding normal tissue and also more accurately detected extraprostatic extension than conventional MRI.[14] DCE-MRI can use as a complimentary tool along with DWI and T2-weighted (T2W) imaging. Jackson et al[15] showed that the sensitivity and specificity of DCE-MRI (50% and 85%, respectively) is higher than that of T2W imaging (21% and 81%, respectively).

Combination of these four MR sequences represents multiparametric MRI (mp-MRI) for diagnosing prostate cancer; however, there is an issue that how many parameters are really required to achieve the best diagnostic accuracy without compromising the workflow in the MR suite. In addition, the updated Prostate Imaging Reporting and Data System (PI-RADS) guideline version 2 published in 2015 by the European Society of Urogenital Radiology (ESUR)[16] has also dropped the use of MRS in routine prostate MRI. This stresses the issue of the optimal sequences of mp-MRI approach.

Therefore, the purpose of this study was to determine the accuracy of each mp-MRI sequences (T2W, DWI, MRS, and DCE-MRI) and their combinations for peripheral zone prostate cancer detection correlation with radical prostatectomy specimens.

Methods

Patients

In this institutional review board-approved study, No. MURA2013/559, we performed a single-institution study of 38 consecutive patients who underwent 1.5-T endorectal MRI before radical prostatectomy from March 1, 2006, to March 31, 2010. Patient age, underlying disease, serum prostate-specific antigen (PSA) level, indication for endorectal MRI, date and type of radical prostatectomy were reviewed from medical records. One experienced urological pathologist reviewed the location and extension of tumor and Gleason score of prostate cancer.

MRI Technique

All prostate MRI examinations were performed by using an endorectal coil (Medrad Inc, Indianola, PA, USA) combined with a four channels Torso array coil in 1.5-T MRI units (Signa HDxt, GE Healthcare, Milwaukee, WI, USA). Immediately before the MRI examination,

all patients underwent intravascular administration of 20 mg hyoscine-n-butylbromide (The Government Pharmaceutical Organization, Thailand) to prevent peristalsis artifacts except when contraindicated.

The MRI protocol included T2-weighted fast spin-echo images, DWI, axial unenhanced T1-weighted, DCE-MRI, and MRS. The imaging protocol are summarized in the supplementary data.

MRI Analysis

One fellowship-trained genitourinary radiologist (P.W.) and one radiologic fellow (S.R.) with 4 and 2 years of experience in prostate MRI, identified prostate cancer lesions on pre-operative mp-MRI. The focal areas with low signal intensity on the T2W images, hyperintensity of diffusion-weighted images corresponding with hypointensity on ADC maps relatived to the rest of the prostate gland were classified as suspicious tumor foci. The locations of tumor detected by T2W images, diffusion weighted/diffusion tensor (DW/DT) images with ADC map and total prostatic volumes were recorded.

The spectra were acquired from a three dimensional magnetic resonance spectroscopic (3D-MRS) imaging data set and scored from pattern I (likely benign) to pattern V (likely malignant) on the basis of prostate cancer metabolism. The peak area choline plus creatine to citrate ratio (CC/C) was calculated.[17] The most representative proton spectral pattern of the two adjacent voxels was recorded.

Dynamic gadolinium enhanced-MRI was analyzed according to three patterns of time-intensity curve (TIC) based on their shapes and time-to-peak.[18, 19] Type 1 (progressive enhancement) was continuous delayed enhancement with no signal peak within 3 minutes. Type 2 (plateau) was intermediate early enhancement with plateauing and a time-to-peak greater than 60 seconds. Type 3 (washout) was rapid enhancement with a time to peak no more than 60 seconds and followed by a rapid wash out of the contrast material.

Histopathologic Analysis

Histopathologic examinations of the all radical prostatectomy specimens were performed by a dedicated genitourinary pathologist (P.C. with 20 years of experience in genitourinary pathology). On each section, individual locations (sides) of tumor, Gleason score, and extent of disease in term of extraprostatic extension were determined. In the discordant findings between radiologist and pathologist, additional pathological reviews were also recorded.

Statistical Analysis

The patient data, MR images and histopathologic data were summarized by mean and standard deviation (SD) for normally distributed continuous variables, median values and ranges for asymmetrical continuous variables and percentage for categorical variables.

The kappa (κ) was used to assess agreement between histopathological and radiological results in terms of location (side) of tumor, presence and location of extracapsular extension and seminal vesicle invasion (SVI). The degrees of agreement was defined from almost perfect agreement (κ = 0.81 - 0.99) to slight agreement (κ = 0.01 - 0.20).

The correlation of T2W, DWI, MRS, and DCE-MRI in differentiation between tumor and non-tumor areas were analyzed by using Pearson's chi-square test or Fisher's exact test. The receiver operating characteristic (ROC) analysis was use to evaluate the accuracy of each mp-MRI sequences (T2W, DWI, MRS, and DCE) and their combinations for peripheral zone prostate cancer localization. All analysis were performed by using STATA version 13 (StataCorp. Version 13. College Station, TX: StataCorp LP; 2013). Statistical significance was defined on the basis of *P* value of less than 0.05.

Results

Patient Characteristics

Thirty-eight men (mean age, 65.67 years; SD, 6.23; range, 48 - 79 years) who underwent endorectal MRI and

subsequent radical prostatectomy with histopathologically proven adenocarcinoma of the peripheral zone of the prostate gland were included. Of these 38 patients, there were 64 tumor areas and 12 non-tumor areas. There are 6 patients had less than 6 weeks duration from core needle biopsy to MRI study date (Table 1).

Histopathologic Findings and Diagnosis

All of the patients in this study had adenocarcinoma of the peripheral zone of prostate gland. Of 76 area of interest, 4 (5.26%) lesions had low grade tumor (Gleason score < 6). Forty two (55.26%) lesions had intermediate grade tumor (Gleason score 6 - 7). Eighteen (23.68%) lesions had high grade tumor (Gleason score 8 - 10).

MRI Findings

The mean total prostatic volume of all 38 patients were 32.09 cc (SD, 13.64; range, 18.59 - 84.85). Twenty-three patients had hypersignal T1-weighted foci of hemorrhage in the peripheral zone. Whereas, 5 of 23 patients had hypersignal T1- weighted foci in the central gland. Seventeen patients had hypersignal T1-weighted foci in the right lobe of prostate gland and 22 patients had hypersignal T1-weighted foci in the left lobe of prostate gland.

T2W Images

All 38 patients underwent T2W images. Sixty (78.94%) areas demonstrated hypointensity on T2W images. There was no demonstrable hypointensity change on T2W in 16 (21.05%) areas. The agreement between hypointensity on T2W and histopathology in terms of presence of tumor was 88.16% (moderate agreement; $\kappa = 0.6$). The sensitivity, specificity, positive predictive value, and negative predictive value were 89.2%, 81.8%, 96.7%, and 56.3%, respectively (Table 2). There were 2 of 60 (3.33%) hypointense T2W areas that negative for malignancy in histopathology specimen. These two areas were ectopic benign prostatic hyperplasia in peripheral zone.

DWI With ADC Map

Twenty-five patients (65.79%) obtained ADC map from DWI sequences, whereas 13 (34.21%) patients obtained from diffusion tensor imaging (DTI) sequences. All of the patients had b values of 500 and 1000 sec/mm^2.

Table 1 Characteristic and Clinical Data of the Patients (N = 38)

Characteristic	No. (%)
Age, mean ± SD (range), y	65.67 ± 6.23 (48 - 79)
Underlying disease	33 (86.84)
Diabetes mellitus	13 (34.21)
Hypertension	26 (68.42)
Dyslipidemia	18 (47.37)
Coronary artery disease	7 (18.42)
Renal impairment	2 (5.26)
Benign prostatic hyperplasia	16 (42.10)
No underlying disease	6 (15.79)
Serum PSA value, mean ± SD (range), ng/mL	29.12 ± 35.80 (3.9 - 179.6)
Duration after biopsy to MRI, mean ± SD (range), d	82.21 ± 75.08 (6 - 301)
Type of radical prostatectomy	38 (100)
Open	6 (15.79)
Laparoscopic	32 (84.2)
Duration after MR study to surgery, mean ± SD (range), d	132.92 ± 203.91 (4 - 1271)

Abbreviation: PSA, prostate-specific antigen; MRI, magnetic resonance imaging; SD, standard deviation.

Table 2 Diagnostic Accuracy of mp-MRI in Prostate Cancer Detection (n = 76)

Parameter	% (95% CI)				DOR	AUC (95% CI)
	Sensitivity	Specificity	PPV	NPV		
T2W	89.2 (79.1 - 95.6)	81.8 (48.2 - 97.7)	96.7 (88.5 - 99.6)	56.3 (29.9 - 80.2)	37.3	0.86 (0.73 - 0.98)
DWI	81.5 (70.0 - 90.1)	90.9 (58.7 - 99.8)	98.1 (90.1 - 100)	45.5 (24.4 - 67.8)	44.2	0.86 (0.76 - 0.96)
MRS pattern III, IV, V*	90.2 (78.6 - 96.7)	100	100	58.3 (27.7 - 84.8)	-	0.95 (0.91 - 0.99)
MRS pattern IV, V*	72.5 (58.3 - 84.1)	100	100	33.3 (14.6 - 57.0)	-	0.86 (0.80 - 0.93)
DCE type 3	38.5 (26.7 - 51.4)	100	100	21.6 (11.3 - 35.5)	-	0.69 (0.63 - 0.75)
DCE type 2, 3	86.2 (75.3 - 93.5)	36.4 (10.9 - 69.2)	88.9 (78.4 - 95.4)	30.8 (9.09 - 61.4)	3.56	0.61 (0.46 - 0.77)
Combination 2 tests						
T2W + DWI	81.5 (70.0 - 90.1)	90.9 (58.7 - 99.8)	98.1 (90.1 - 100)	45.5 (24.4 - 67.8)	44.2	0.86 (0.76 - 0.96)
T2W + MRS IV, V*	70.6 (56.2 - 82.5)	100	100	31.8 (13.9 - 54.9)	-	0.85 (0.79 - 0.92)
T2W + MRS III, IV, V*	84.3 (71.4 - 93.0)	100	100	46.7 (21.3 - 73.4)	-	0.92 (0.87 - 0.97)
T2W + DCE type 2, 3	78.5 (66.5 - 87.7)	81.8 (48.2 - 97.7)	96.2 (87.0 - 99.5)	39.1 (19.7 - 61.5)	16.4	0.80 (0.67 - 0.93)
DWI + DCE type 2, 3	73.8 (61.5 - 84.0)	90.9 (58.7 - 99.8)	98 (89.1 - 99.9)	37 (19.4 - 57.6)	28.2	0.82 (0.72 - 0.93)
DWI + MRS III, IV, V*	78.4 (64.7 - 88.7)	100	100	38.9 (17.3 - 64.3)	-	0.89 (0.84 - 0.95)
DWI + MRS IV, V*	64.7 (50.1 - 77.6)	100	100	28 (12.1 - 49.4)	-	0.82 (0.76 - 0.89)
DCE type 2, 3 + MRS III, IV, V*	76.5 (62.5 - 87.2)	100	100	36.8 (16.3 - 61.6)	-	0.88 (0.82 - 0.94)
DCE type 2, 3 + DWI + MRS IV, V*	58.8 (44.2 - 72.4)	100	100	25 (10.7 - 44.9)	-	0.79 (0.73 - 0.86)
Combination 3 tests						
T2W + DWI + MRS IV, V*	64.7 (50.1 - 77.6)	100	100	28 (12.1 - 49.4)	-	0.82 (0.76 - 0.89)
T2W + DWI + MRS III, IV, V*	78.4 (64.7 - 88.7)	100	100	38.9 (17.3 - 64.3)	-	0.89 (0.84 - 0.95)
T2W + DWI + DCE type 2, 3	73.8 (61.5 - 84.0)	90.9 (58.7 - 99.8)	98.0 (89.1 - 99.9)	37.0 (19.4 - 57.6)	28.2	0.82 (0.72 - 0.93)
(2/3)[a] T2W + DWI + MRS IV, V*	88.2 (76.1 - 95.6)	100	100	53.8 (25.1 - 80.8)	-	0.94 (0.90 - 0.99)
(2/3)[a] T2W + DWI + MRS III, IV, V*	88.2 (76.1 - 95.6)	100	100	53.8 (25.1 - 80.8)	-	0.94 (0.90 - 0.99)
(2/3)[a] T2W + DWI + DCE type 2, 3	86.2 (75.3 - 93.5)	81.8 (48.2 - 97.7)	96.6 (88.1 - 99.6)	50.0 (26.0 - 74.0)	28.0	0.84 (0.71 - 0.97)
Combination 4 tests						
T2W + DWI + MRS IV, V* + DCE type 2, 3	54.9 (40.3 - 68.9)	100	100	23.3 (9.93 - 42.3)	-	0.78 (0.71 - 0.84)
T2W + DWI + MRS III, IV, V* + DCE type 2, 3	68.6 (54.1 - 80.9)	100	100	30.4 (13.2 - 52.9)	-	0.84 (0.78 - 0.91)
(2/4)[a] T2W + DWI + MRS IV, V* + DCE type 2, 3	92.2 (81.1 - 97.8)	85.7 (42.1 - 99.6)	97.9 (88.9 - 99.9)	60.0 (26.2 - 87.8)	70.5	0.89 (0.74 - 1.00)
(2/4)[a] T2W + DWI + MRS III, IV, V* + DCE type 2, 3	96.1 (86.5 - 99.5)	85.7 (42.1 - 99.6)	98 (89.4 - 99.9)	75 (34.9 - 96.8)	147	0.90 (0.77 - 1.00)
(3/4)[a] T2W + DWI + MRS IV, V* + DCE type 2, 3	84.3 (71.4 - 93.0)	100	100	46.7 (21.3 - 73.4)	-	0.92 (0.87 - 0.97)
(3/4)[a] T2W + DWI + MRS III, IV, V* + DCE type 2, 3	84.3 (71.4 - 93.0)	100	100	46.7 (21.3 - 73.4)	-	0.92 (0.87 - 0.97)

Abbreviation: AUC, area under the ROC curve; CI, confidence interval; DCE, dynamic contrast-enhanced; DWI, diffusion-weighted imaging; MRS, magnetic resonance spectroscopic; NPV, negative predictive value; DOR, diagnostic odds ratio; PPV, positive predictive value; T2W, T2-weighted.

* Total number of lesions for MRS analysis was 58 (n = 58) because exclusion of poor metabolic spectra quality.

[a] The combination test of mp-MRI (T2W, DWI, MRS, and DCE-MRI) was (2/3), positive 2 in 3 tests; (2/4), positive 2 in 4 tests; and (3/4), positive 3 in 4 tests.

There were 54 of 76 (71.05%) areas of restricted diffusion in the peripheral zone. Twenty-two (28.94%) areas were not visible focal area of restricted diffusion by DWI with ADC map. The sensitivity, specificity, positive predictive value and negative predictive value of DWI were 81.5%, 90.9%, 98.1%, and 45.5%, respectively. One of 54 (0.02%) area of hyperintense DWI image with corresponding hypointensity on ADC maps had no malignancy in histopathology specimen. This area was benign prostatic hyperplasia. DWI and histopathology had 82.89% agreement in term of presence of tumor and location (side) of tumor.

MRS Image

All 76 tumor and non-tumor areas were analyzed according to 5 patterns of representative spectra. Eighteen areas were excluded from MRS analysis due to marked lipid contamination, presence of misalignment of metabolic resonance peak, and inability to classify into five categories. Two in 7 areas of pattern I had tumor. Three in 5 areas of pattern II had tumor. All 9 of pattern III areas had tumor. All 13 of pattern IV areas had tumor. Twenty-three in 24 of pattern V areas had tumor.

We divided positive malignant spectral patterns in to two groups: first group included pattern III, IV, and V (46 of 58, 79.31%), and second group included pattern IV and V (37 of 58, 63.79%). The sensitivity, specificity, positive predictive value and negative predictive value as well as the area under the ROC curve (AUC) for tumor localization of combined spectral patterns were shown in Table 2.

DCE-MR Image

All 38 patients (64 tumor and 12 non-tumor areas) were analyzed according to 3 patterns of dynamic time-intensity curve.[19,20] Thirteen areas had dynamic curve type 1 (progressive enhancement). Thirty-eight areas had dynamic curve type 2 (plateau). Twenty-five areas had dynamic curve type 3 (washout). No dynamic curve pattern 3 was seen in all 12 non-tumor areas. Seven non-tumor areas showed dynamic curve type 2. There was 52.56% agreement between DCE-MR images and histopathology in term of presence of tumor.

We divided positive dynamic curve pattern into two groups; first group included curve type 2 and 3 (63 of 76, 82.89%), and second group included only type 3 curve (25 of 76, 32.89%). The sensitivity, specificity, positive predictive value and negative predictive value as well as AUC for tumor localization of dynamic curve pattern were shown in Table 2.

Correlation Between mp-MRI and Histopathology

The mp-MRI (combined T2W, DWI, MRS, and DCE-MRI) and histopathology correlation was shown in Table 2. Our study showed highest accuracy for tumor detection when combined T2W+MRS (pattern III, IV, V) with AUC 0.92. The AUC of combined T2W+DWI, T2W+MRS (pattern IV, V), and T2W+DCE (curve type 2, 3) were 0.86, 0.85, and 0.80, respectively. For combination of 3 and 4 tests, the AUC were 0.89 for T2W+DWI+MRS, 0.82 for T2W+DWI+DCE, and 0.84 for T2W+DWI+MRS+DCE. The accuracy was higher when using positive 2 in 3 tests of T2W+DWI+MRS (AUC 0.94) than using positive all 3 tests of T2W+DWI+MRS (AUC 0.89). The accuracy also was higher when using positive 3 in 4 tests of T2W+DWI+MRS+DCE (AUC 0.92) than using positive 2 in 4 tests (AUC 0.90) or positive all 4 tests of T2W+DWI+MRS+DCE (AUC 0.84).

There were no statistically significant differences between the AUC of T2W, T2W + DWI, T2W + DWI + DCE, and T2W + DWI + MRS, as well as T2W+DWI+MRS+DCE. The highest AUC curve was T2W + DWI (0.86) ($P = 0.08$).

A mp-MRI example case of a highly suspicious for prostate cancer in the right base to mid peripheral zone is shown in Figure 1.

Discussion

Our study showed that both T2WI and DWI demonstrate moderate agreement with histopathology in term of presence of peripheral zone prostate cancer. It is well documented that prostate cancer in peripheral zone shows hypointensity on T2W images in contrast to normal hyperintensity on T2W of background peripheral zones. In addition, prostate cancer that has increased cellular

density and an excess of intra-and intercellular membranes compared with normal glandular tissue results in restricted diffusion on DWI.[21] However, the presence of hypointense T2W lesion is not specific for malignancy, some negative for malignancy in histopathology; these areas show benign prostatic hyperplasia in our study. There are also multiple other conditions that mimics prostate cancer on T2W images in peripheral zone such as hemorrhage, prostatitis, scarring, atrophy, and effects of radiation therapy, cryosurgery, or hormonal therapy.[22]

Previous studies have shown that DWI can help differentiate between malignant and benign prostatic tissue seen as a focal area of marked hyperintensity on DWI at high b values and marked hypointensity on ADC map (lower ADC value) of prostate cancer compared with normal tissue.[23-25] In our study, DWI yielded the same area under the ROC curve as compared with T2W (0.86), however, DWI yielded better specificity than T2W (90.9% vs 81.8%) corresponding with the previously report area under the ROC, sensitivity, and specificity of 0.85, 69%, and 89%, respectively.[26] It was also shown in our study that combination of T2W+DWI achieved high accuracy with AUC (0.86) and higher than other combinations [T2W+DWI+DCE (0.82), T2W+DWI+MRS (0.81), or T2W+DWI+DCE+MRS (0.78)]. These findings were indicated that DWI was seems to be the most important MR sequence and could be a useful complementary sequence to conventional anatomic imaging for prostate cancer identification corresponding with previous studies.[26-28] Therefore, in updated PI-RADS version 2[16] recommends using DWI and ADC map as the primary sequence for diagnosing peripheral zone prostate cancer.

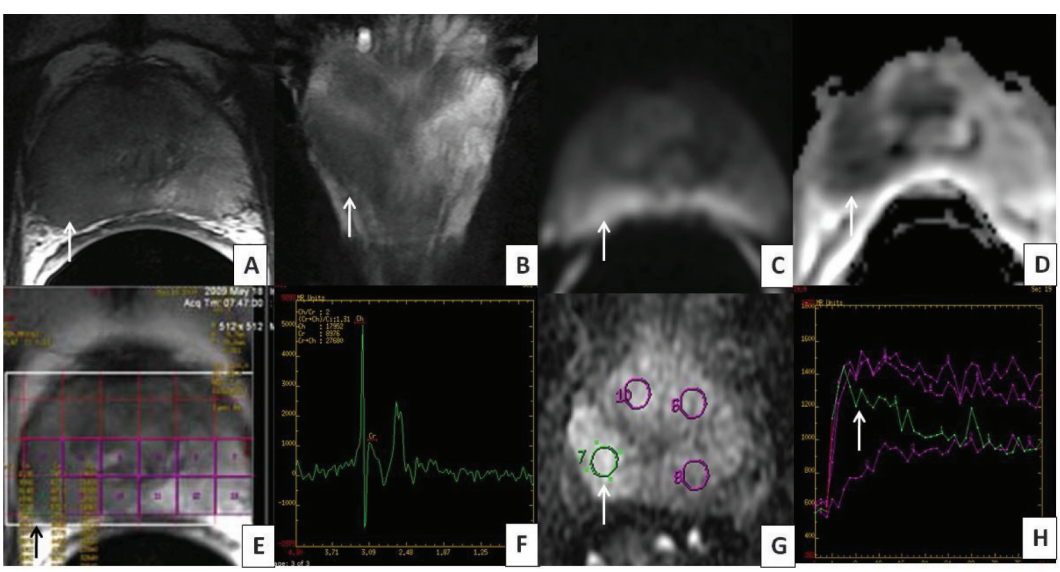

Figure 1 *Multiparametric MRI of Peripheral Zone Prostate Cancer (Gleason Score 4+3) in a 76-Year-Old Patient With High Serum Prostate Specific Antigen (61.03 ng/mL)*

Thin-sliced axial (A) and coronal (B) T2-weighted image shows focal hypointense lesion at right base to mid-peripheral zone (arrows) with focal bulging and disruption of the overlying capsule. Diffusion-weighted images (DWI) (C) with ADC map (D) at b values of 1000 s/mm^2 show an area of restricted diffusion at right base to mid-peripheral zone. Three dimensional (3D) MRS voxel and metabolic pattern (E, F) show likely malignant (pattern V) in area corresponds to hypointense lesion on T2W. Dynamic contrast-enhanced (DCE) MRI (G) and time signal intensity curve (H) show high wash-in with rapid wash-out (type 3 curve) in area corresponds to hypointense lesion on T2-weighted image.

Even though, our study showed that MRS (pattern III, IV, V) achieved highest accuracy for tumor detection for single parameter with sensitivity 90.2% and specificity 100%; AUC 0.95 as compared with a previously reported sensitivity and specificity of approximately 64% - 93% and 69.2% - 89.3%.[17, 29] There was also highest accuracy when combined T2W+MRS (pattern III, IV, V) as compared with the other two combination parameters with sensitivity 84.3% and specificity 100%; AUC 0.92. Unfortunately, 24% (18/76) of lesions in this study were excluded from MRS analysis due to poor metabolic spectra quality. This reason may cause overestimate accuracy of MRS as compared with the other parameters. According to aforementioned complex interpretation and limited reproducibility of MRS as well as long acquisition time, the role of MRS is still under debate[30] and still not considered for the first imaging parameter for mp-MRI of the prostate gland.

For dynamic contrast-enhanced MR image (DCE), the highest specificity (100%) was achieved in this study with Type 3 curve (washout), however, the sensitivity was poor (38.5%). By combining Type 2 and 3 curves as positive DCE result, the sensitivity was increased to 86.2%, but compromises the specificity (36.4%). Therefore, the interpretation of time-intensity curve patterns might be limited in clinical practice. In updated PI-RADS version 2 guideline, DCE images curve analysis was downgraded and only interpreted as positive or negative enhancement.[16] It is also should be mentioned that parenchymal enhancement can be seen in prostatitis and in highly vascularized BPH nodules,[27] these may cause limitation of using this sequence as the primary sequence in tumor localization. However, DCE is still beneficial in identification of extraprostatic extension[14] and in the update PI-RADS version 2 still recommended to include DCE in all prostate mp-MRI exams so as not to miss some small significant cancers.[16]

There was no significant benefit of combination tests more than two tests or additional benefit more than T2W+DWI for tumor detection in this study. In contrast to a previous report that showed T2W+DWI+DCE to achieve highest accuracy. The use of combination more than two tests achieved higher AUC in high grade peripheral zone cancer than those performed ≤ 2 MR sequences.[31] The difference result is probably due to relative subjective for imaging interpretation and disproportional number of tumor aggressiveness in this study. Further use of standard diagnostic terminology and level of suspicious for imaging interpretation may reduce variability in imaging interpretation especially in multiparametric prostate MRI.

The reliability of the present study was limited by retrospective study design and relatively small sample size. Also, there was disproportional number of patients in different tumor grading, the relationship between tumor and non-tumor areas may therefore be weak. Secondly, the radiologist was not blinded to histopathological findings when assessing spectra and dynamic perfusion curve. Thirdly, the intra- and inter-observer variabilities could not be measured because the study was based on consensus of two radiologists. Finally, the slice level in MR images could not be matched exactly with that of histopathology, only side (lobe) of prostate gland was compared.

Conclusions

DWI was the most useful complementary sequence to conventional anatomical T2W imaging for prostate cancer foci identification. The 3D-MRS and DCE-MR images may be use as confirmation tools in tumor detection of peripheral zone prostate cancer under its limitations.

Supplement

MRI Technique

After the acquisition of localizing images, sagittal, coronal, axial thin-slice T2-weighted fast spin-echo images through the prostate gland and seminal vesicles were obtains using the following parameter: TR range/TE, 3000 - 6000/104; echo-train length (ETL), 18; FOV, 16 cm; section thickness/gab, 3/0 mm; matrix, 512 × 256; and number of excitation (NEX), 4. The transverse axial T1-weighted fast spine echo images with a TR/TE of 400 - 600/10 - 15; matrix, 320 × 224;

and all other parameters matched to the axial thin-sliced T2-weighted fast spin-echo sequence were obtained. The axial thin-slice T2-weighted images were used for calculate prostatic volume by Functool package post processing with the GE Advantage Workstation (GE Medical Systems, Milwaukee, WI, USA)

For the DWI sequence, echo-planar imaging was used with the following parameters: TR/TE, 3000 - 6000/60 - 120; FOV, 18 × 18; section thickness/gab, 5/1 mm; matrix 128 × 128; and NEX, 6. The axial free-breathing DTI was performed in 8 patients of this study using a TR of 8000 - 9000 milliseconds and all other parameters matched to the DWI. ADC values were obtained from the DWI/DTI sequences, which performed with b values of 100, 250, 500, 750, 1000, and 2000 s/mm^2. The ADC maps were generated by auto-calculation of the ADC value in each pixel of each slice.

MRS was performed in all patients using the endorectal coil, 3D chemical shift imaging spin-echo sequence and water- and fat suppressed acquisition with the following parameters: TR/TE, 1000/130; 4 averages; A point-resolved spectroscopy sequence (PRESS) was used to acquire the proton magnetic resonance spectroscopy (^{1}H-MRS) from a volume of interest closely around the prostate. The nominal voxel size was 0.45 cm^3. Six spatially selective saturation bands were interactively positioned around the volume of interest for outer volume lipid suppression. The total scanning time was 17 minutes including the voxel prescription, shimming, and prescan optimization. The full width at half maximum (FWHM) of the water peak ranges from 5 - 7 Hz with 97% - 99% water suppression. The MRS post-processing was used to evaluate the integral ratios of choline plus creatine to citrate. Each spectral signal was zero filled to 1024 data points and multiplied by a Hamming filter. Fourier transformation, phase and frequency adjustment, as well as baseline correction and calculation of choline plus creatine to citrate ratio were automatically performed.

A dynamic view-sharing time-resolved angiography with stochastic trajectories gradient-echo T1-weighted sequence was performed over 5 minutes by a 0.1 mmol/kg bolus of gadolinium-based contrast agent injection at a rate of 3 mL/s, followed by a 30 mL saline flush at the same rate. Serial T1-weighted 3D images were obtained every 12 seconds through the entire prostate, using an MR-compatible automated injector (Medrad Inc, Indianola, PA, USA). A fast saturation-recovery TurboFLASH (fast low angle shot) sequence was performed with the following parameters; TR/TE, 4.1/1.9; flip angle, 12°; FOV, 20 × 24; matrix, 256 × 192; slice thickness, 5 mm; and a distance factor of 0.2 or higher (adaptation to individual prostate size) was acquired with a temporal resolution of four slices per second. MR perfusion data were transferred to a separate workstation. Areas with low signal intensity on the T2W images represent suspicious prostate lesion. At least one slice of the stack was positioned at the level of the largest extent of the respective lesion.

References

1. Siegel RL, Miller KD, Jemal A. Cancer statistics, 2015. *CA Cancer J Clin.* 2015;65(1):5-29. doi:10.3322/caac.21254.
2. Rosenkrantz AB, Deng FM, Kim S, et al. Prostate cancer: multiparametric MRI for index lesion localization--a multiple-reader study. *AJR Am J Roentgenol.* 2012;199(4):830-837. doi:10.2214/AJR.11.8446.
3. Wetter A, Engl TA, Nadjmabadi D, et al. Combined MRI and MR spectroscopy of the prostate before radical prostatectomy. *AJR Am J Roentgenol*. 2006;187(3):724-730. doi:10.2214/AJR.05.0642.
4. Hricak H. MR imaging and MR spectroscopic imaging in the pre-treatment evaluation of prostate cancer. *Br J Radiol*. 2005;78:S103-S111. doi:10.1259/bjr/11253478.
5. Caivano R, Cirillo P, Balestra A, et al. Prostate cancer in magnetic resonance imaging: diagnostic utilities of spectroscopic sequences. *J Med Imaging Radiat Oncol.* 2012;56(6):606-616. doi:10.1111/j.1754-9485.2012.02449.x.

6. Barentsz JO, Weinreb JC, Verma S, et al. Synopsis of the PI-RADS v2 guidelines for multiparametric prostate magnetic resonance imaging and recommendations for use. *Eur Urol.* 2016;69(1):41-49. doi:10.1016/j.eururo.2015.08.038.
7. Hambrock T, Somford DM, Huisman HJ, et al. Relationship between apparent diffusion coefficients at 3.0-T MR imaging and Gleason grade in peripheral zone prostate cancer. *Radiology*. 2011;259(2):453-461. doi:10.1148/radiol.11091409.
8. Rosenkrantz AB, Mannelli L, Kong X, et al. Prostate cancer: utility of fusion of T2-weighted and high b-value diffusion-weighted images for peripheral zone tumor detection and localization. *J Magn Reson Imaging.* 2011;34(1): 95-100. doi:10.1002/jmri.22598.
9. Haider MA, van der Kwast TH, Tanguay J, et al. Combined T2-weighted and diffusion-weighted MRI for localization of prostate cancer. *AJR Am J Roentgenol.* 2007;189(2):323-328. doi:10.2214/AJR.07.2211.
10. Lim HK, Kim JK, Kim KA, Cho KS. Prostate cancer: apparent diffusion coefficient map with T2-weighted images for detection - a multireader study. *Radiology.* 2009;250(1):145-151. doi:10.1148/radiol.2501080207.
11. Wibulpolprasert P, Phongkitkarun S, Chalermsanyakorn P. Clinical applications of diffusion-weighted-MRI in prostate cancer. *J Med Assoc Thai.* 2013;96(8):967-975.
12. Nagarajan R, Margolis D, Raman S, et al. Correlation of Gleason scores with diffusion-weighted imaging findings of prostate cancer. *Adv Urol.* 2012;2012:374805. doi:10.1155/2012/374805.
13. Mucci LA, Powolny A, Giovannucci E, et al. Prospective study of prostate tumor angiogenesis and cancer-specific mortality in the health professionals follow-up study. *J Clin Oncol.* 2009;27(33):5627-5633. doi:10.1200/JCO.2008.20.8876.
14. Ogura K, Maekawa S, Okubo K, et al. Dynamic endorectal magnetic resonance imaging for local staging and detection of neurovascular bundle involvement of prostate cancer: correlation with histopathologic results. Urology. 2001;57(4): 721-726. doi:10.1016/S0090-4295(00)01072-4.
15. Jackson AS, Reinsberg SA, Sohaib SA, et al. Dynamic contrast-enhanced MRI for prostate cancer localization. *Br J Radiol.* 2009;82(974):148-156. doi:10.1259/bjr/89518905.
16. Weinreb JC, Barentsz JO, Choyke PL, et al. PI-RADS prostate imaging - reporting and data system: 2015, version 2. *Eur Urol*. 2016;69(1):16-40. doi:10.1016/j.eururo.2015.08.052.
17. Jung JA, Coakley FV, Vigneron DB, et al. Prostate depiction at endorectal MR spectroscopic imaging: investigation of a standardized evaluation system. *Radiology.* 2004;233(3):701-708. doi:10.1148/radiol.2333030672
18. Johnson LM, Turkbey B, Figg WD, Choyke PL. Multiparametric MRI in prostate cancer management. *Nat Rev Clin Oncol.* 2014;11(6):346-353. doi:10.1038/nrclinonc.2014.69.
19. Ito H, Kamoi K, Yokoyama K, Yamada K, Nishimura T. Visualization of prostate cancer using dynamic contrast-enhanced MRI: comparison with transrectal power Doppler ultrasound. *Br J Radiol.* 2003;76(909):617-624. doi:10.1259/bjr/52526261.
20. Scherr MK, Seitz M, Müller-Lisse UG, Ingrisch M, Reiser MF, Müller-Lisse UL. MR-perfusion (MRP) and diffusion-weighted imaging (DWI) in prostate cancer: quantitative and model-based gadobenate dimeglumine MRP parameters in detection of prostate cancer. *Eur J Radiol.* 2010;76(3):359-366. doi:10.1016/j.ejrad.2010.04.023.
21. Malayeri AA, El Khouli RH, Zaheer A, et al. Principles and applications of diffusion-weighted imaging in cancer detection, staging, and treatment follow-up. *Radiographics*. 2011;31(6):1773-1791. doi:10.1148/rg.316115515.
22. Bonekamp D, Jacobs MA, El-Khouli R, Stoianovici D, Macura KJ. Advancements in MR imaging of the prostate: from diagnosis to interventions. *Radiographics.* 2011;31(3):677-703. doi:10.1148/rg.313105139.
23. Pickles MD, Gibbs P, Sreenivas M, Turnbull LW. Diffusion-weighted imaging of normal and malignant prostate tissue at 3.0T. *J Magn Reson Imaging*. 2006;23(2):130-134. doi:10.1002/jmri.20477.

24. Kumar V, Jagannathan NR, Kumar R, et al. Apparent diffusion coefficient of the prostate in men prior to biopsy: determination of a cut-off value to predict malignancy of the peripheral zone. *NMR Biomed.* 2007;20(5):505-511. doi:10.1002/nbm.1114.
25. desouza NM, Reinsberg SA, Scurr ED, Brewster JM, Payne GS. Magnetic resonance imaging in prostate cancer: the value of apparent diffusion coefficients for identifying malignant nodules. *Br J Radiol*. 2007;80(950):90-95. doi:10.1259/bjr/24232319.
26. Tan CH, Wei W, Johnson V, Kundra V. Diffusion-weighted MRI in the detection of prostate cancer: meta-analysis. *AJR Am J Roentgenol.* 2012;199(4):822-829. doi:10.2214/AJR.11.7805.
27. Ghai S, Haider MA. Multiparametric-MRI in diagnosis of prostate cancer. *Indian J Urol.* 2015;31(3):194-201. doi:10.4103/0970-1591.159606.
28. Osugi K, Tanimoto A, Nakashima J, et al. What is the most effective tool for detecting prostate cancer using a standard MR scanner? *Magn Reson Med Sci.* 2013;12(4):271-280. doi:10.2463/mrms.2012-0054.
29. Bhatia C, Phongkitkarun S, Booranapitaksonti D, Kochakarn W, Chaleumsanyakorn P. Diagnostic accuracy of MRI/MRSI for patients with persistently high PSA levels and negative TRUS-guided biopsy results. *J Med Assoc Thai.* 2007;90(7):1391-1399.
30. Martin Noguerol T, Sanchez-Gonzalez J, Martinez Barbero JP, Garcia-Figueiras R, Baleato-Gonzalez S, Luna A. Clinical imaging of tumor metabolism with ^{1}H magnetic resonance spectroscopy. *Magn Reson Imaging Clin N Am.* 2016;24(1):57-86. doi:10.1016/j.mric.2015.09.002.
31. Schimmöller L, Quentin M, Arsov C, et al. MR-sequences for prostate cancer diagnostics: validation based on the PI-RADS scoring system and targeted MR-guided in-bore biopsy. *Eur Radiol.* 2014;24(10):2582-2589. doi:10.1007/s00330-014-3276-9.

Original Article/นิพนธ์ต้นฉบับ

ความถูกต้องแม่นยำของพารามิเตอร์ต่างๆ ที่ได้จากการตรวจด้วยคลื่นแม่เหล็กไฟฟ้า ในการวินิจฉัยโรคมะเร็งต่อมลูกหมากบริเวณชั้นนอก

พรพรรณ วิบุลผลประเสริฐ[1], ศศิประภา รงค์ทอง[1], สิทธิ์ พงษ์กิจการุณ[1], พนัส เฉลิมแสนยากร[2]

[1] ภาควิชารังสีวิทยา คณะแพทยศาสตร์โรงพยาบาลรามาธิบดี มหาวิทยาลัยมหิดล

[2] ภาควิชาพยาธิวิทยา คณะแพทยศาสตร์โรงพยาบาลรามาธิบดี มหาวิทยาลัยมหิดล

บทคัดย่อ

บทนำ: พารามิเตอร์ต่างๆ ที่ได้จากการตรวจด้วยคลื่นแม่เหล็กไฟฟ้า (Multiparametric magnetic resonance imaging, mp-MRI) ซึ่งเป็นการตรวจที่ไม่รุกล้ำร่างกายผู้ป่วยที่ดีที่สุดสำหรับการตรวจ การประเมินความรุนแรง การประเมินระยะของโรค และการระบุตำแหน่งสำหรับการเจาะพิสูจน์ชิ้นเนื้อของโรคมะเร็งต่อมลูกหมาก การตรวจสอบความถูกต้องแม่นยำของพารามิเตอร์ต่างๆ จึงมีความสำคัญอย่างยิ่งในทางคลินิก

วัตถุประสงค์: เพื่อศึกษาความถูกต้องแม่นยำของพารามิเตอร์ต่างๆ ที่ได้จากการตรวจด้วยคลื่นแม่เหล็กไฟฟ้า ได้แก่ T2-weighted imaging (T2W), Diffusion-weighted imaging (DWI), 3D spectroscopic (3D-MRS) และ Dynamic contrast-enhanced (DCE) ในการวินิจฉัยโรคมะเร็งต่อมลูกหมากบริเวณชั้นนอก (Peripheral zone)

วิธีการศึกษา: การศึกษาย้อนหลังในกลุ่มตัวอย่างผู้ป่วยโรคมะเร็งต่อมลูกหมากบริเวณชั้นนอก จำนวน 38 คน ที่ได้รับการตรวจด้วยคลื่นแม่เหล็กไฟฟ้าก่อนการผ่าตัด ระหว่างเดือนมีนาคม พ.ศ. 2549 ถึงเดือนมีนาคม พ.ศ. 2553 โดยประเมินความสามารถของพารามิเตอร์ดังกล่าวในการแยกความต่างบริเวณที่เป็นมะเร็งกับบริเวณที่ไม่เป็นมะเร็ง การวิเคราะห์ข้อมูลใช้สถิติ Pearson's chi-square test และ Fisher's exact test และใช้การวิเคราะห์ Receiver operating characteristic (ROC) เพื่อประเมินความถูกต้องแม่นยำในการวินิจฉัยโรคมะเร็งต่อมลูกหมาก

ผลการศึกษา: จากรอยโรค 76 ตำแหน่ง ในกลุ่มตัวอย่างผู้ป่วย ค่า AUC (Area under the ROC curve) ในการวินิจฉัยโรคมะเร็งต่อมลูกหมาก เท่ากับ 0.86 (T2W), 0.86 (DWI), 0.95 (MRS) และ 0.61 (DCE) ค่า AUC ของ T2W+DWI, T2W+MRS และ T2W+DCE เท่ากับ 0.86, 0.92, และ 0.80 ตามลำดับ และค่า AUC ของ T2W+DWI, T2W+DWI+DCE, T2W+DWI+MRS และ T2W+DWI+MRS+DCE เท่ากับ 0.86, 0.82, 0.81, และ 0.78 ตามลำดับ ซึ่งไม่พบความแตกต่างกันอย่างมีนัยสำคัญทางสถิติ

สรุป: พารามิเตอร์ DWI เป็นพารามิเตอร์เสริมที่มีประโยชน์ที่สุด รองจากพารามิเตอร์ T2W ซึ่งใช้เป็นพื้นฐานสำหรับการวินิจฉัยโรคมะเร็งต่อมลูกหมาก อย่างไรก็ตาม พารามิเตอร์ 3D-MRS และ DCE อาจช่วยสนับสนุนการยืนยันตำแหน่งของโรคมะเร็งต่อมลูกหมากได้

คำสำคัญ: มะเร็งต่อมลูกหมาก บริเวณชั้นนอก พารามิเตอร์ที่ได้จากการตรวจด้วยคลื่นแม่เหล็กไฟฟ้า ความถูกต้องแม่นยำในการวินิจฉัย

Corresponding Author: พรพรรณ วิบุลผลประเสริฐ
ภาควิชารังสีวิทยา คณะแพทยศาสตร์โรงพยาบาลรามาธิบดี มหาวิทยาลัยมหิดล
270 ถนนพระรามที่ 6 แขวงทุ่งพญาไท เขตราชเทวี กรุงเทพฯ 10400
โทรศัพท์ +66 2201 1212 โทรสาร +66 2201 1297 อีเมล punlee77@gmail.com, pornphan.wib@mahidol.ac.th